JOURNAL OF MATERIALS SCIENCE 30 (1995) 6370–6376

Effects of surface oxide layers on crack initiation and growth of HSLA steel under cyclic loading in air and in ultrahigh vacuum

Y. W. CHUNG
Department of Materials Science and Engineering, Northwestern University, Evanston, IL 60201, USA

W. J. LEE
Department of Electronic Materials Engineering, Korea Advanced Institute of Science and Technology, Taejon, 305-701, Korea

Effects of the thermally grown wustite on the fatigue crack initiation and growth in HSLA steel are evaluated as a function of oxide thickness, strain amplitude, and gaseous environment in the push–pull plastic strain control mode, with special attention being given to the early stage of microcrack initiation. Specimens with a wustite surface layer thermally grown to 0.2 and 0.6 μm thicknesses show predominantly intergranular cracking at plastic strain amplitudes of 5×10^{-4} and 1×10^{-3} both in air and in ultrahigh vacuum (UHV), in contrast to the as-polished specimens where slip band cracking is the favoured mode. The cracking mode in the oxide layer is discussed in terms of the strain amplitude and the dislocation behaviour near the oxide/metal interface. The features of microcrack initiation in the oxide layer is not affected by the gaseous environment. Once, however, the surface oxide fractures, the rate of crack growth through the base metal is greatly reduced in UHV.

1. Introduction

The formation of a brittle oxide layer on a metallic crystal can modify not only chemical activity of the surface but also its mechanical properties [1, 2]. In commercial hot-rolled steel products like high strength low alloy (HSLA) steel, an oxide layer forms and remains in many applications throughout the manufacturing and the in-service life of many components. Since HSLA sheet steels are used in many structural applications involving cyclic loading (for example, in the automotive industry), a knowledge of their fatigue behaviour is important. Since fatigue cracks generally initiate from the surface, the nature and the extent of the oxide layer are expected to influence the fatigue properties. Fatigue cracking in an oxide/metal composite specimen is a complex process which depends on a variety of factors: elastic properties of the oxide, structures of the oxide and the substrate, epitaxial relationship between the oxide and the substrate, interfacial energy, oxide thickness, morphology of the oxide, strain or stress amplitude, frequency, temperature, and environment.

It has been known since the pioneering work of Gough and Sopwith [3, 4] that the fatigue resistance of metals increases as the ambient pressure decreases and that this greater fatigue resistance in vacuum is due to the absence of chemically active gases such as oxygen and water vapour. There has been a number of investigations addressing the influence of gaseous environments from various points of view (see [5–7] for a review). Fatigue tests were performed in vacuum in order to eliminate environmental effects. However, the vacuum employed by most investigators was not lower than 1×10^{-4} Pa. At these pressures, an initially clean surface can be contaminated within a few seconds (assuming sticking probability of unity), and this may affect the fatigue properties in a major way. Working with commercially pure iron, Majumdar and Chung [8] found that an oxygen pressure on the order of 10^{-4} Pa is sufficient to cause distinct environmental effects on cyclic surface deformation and crack initiation. Therefore, a superior degree of vacuum is required in order to eliminate all of the gaseous environmental effects.

The fatigue process is often roughly divided into the phases of crack initiation and crack propagation [9–11]. Understanding the mechanism of initiation and early growth of microcracks is essential for improved prediction of the fatigue life. However, most of environment-related fatigue studies in the past have been directed towards the crack propagation stage and relatively little attention has been paid to the crack initiation stage. In the present research, effects of the surface oxide layer on the fatigue crack initiation and growth in HSLA steel are evaluated as a function of the oxide thickness (0.2 and 0.6 μm), plastic strain amplitude (5×10^{-4} and 1×10^{-3}), and gaseous environment (air, ultrahigh vacuum) in the push–pull plastic strain control mode, with special attention being given to the early stage of microcrack initiation. The

0022–2461

results are compared with those obtained in the as-polished specimens under the same test conditions.

2. Experimental procedures

A commercial hot-rolled HSLA steel plate used in this research was provided by the Inland Steel Company Research Laboratory and was found to contain 0.11 wt % Nb. Controlled thermomechanical processing was employed to obtain a fine grain size (~7 μm) and a fine dispersion of Nb carbo-nitride precipitates in the ferrite matrix. The mechanical properties have been documented elsewhere, useful to give yield and tensile stresses, and elongation [12]. Sheet-type fatigue specimens were machined with the loading axis parallel to the rolling direction. They were subsequently polished to a 0.25 μm diamond finish. A stable, adherent oxide layer was produced on the polished specimens by oxidizing in an atmosphere of CO/CO_2 mixed in the ratio of 1 to 1.45 at 627 °C. The composition of the oxide layer was characterized by Auger electron spectroscopy (AES) analysis. The linear relationship [13] between the Auger peak-to-peak height ratio of O (510 eV)/Fe (598 eV) and the oxygen-to-iron atomic ratio in the oxide was used as a calibration curve. The iron oxide produced on the HSLA steel was identified as a wustite having a composition of $Fe_{0.94}O$. The thickness of the oxide layer was controlled by varying the oxidation time. The average thickness was determined from the measured weight-gain and the known density of the wustite. A direct measurement was also made using a scanning electron microscope (SEM).

An axial-loading electrohydraulic fatigue apparatus was installed in an ultrahigh vacuum (UHV) scanning Auger microprobe (SAM) equipped with Auger analysis, ion sputtering, secondary electron imaging, and controlled gas admittance capabilities. A detailed description of the apparatus and electronics has been presented elsewhere [14]. All fatigue experiments were done with this apparatus under plastic strain controlled cycling using a triangular strain waveform and a constant total strain rate of 1×10^{-3} s^{-1} (except for UHV tests where the strain rate was 1×10^{-3} s^{-1} for the first 50 000 cycles and 5×10^{-3} s^{-1} thereafter due to the long fatigue life).

Fully reversed push–pull strain cycling was performed at a constant plastic strain amplitude ($\Delta\varepsilon_p/2$) of 5×10^{-4} with polished and oxidized (with a 0.2 μm thick wustite) surfaces both in air and in UHV (6.5×10^{-8} Pa). Observations of the surface deformation was made through TEM (two-stage surface replication method) and/or SEM examination. Microcrack initiation life N_i was defined as the number of cycles in the fatigue sequence required to generate a microcrack which is detectable under TEM or SEM examination. The smallest, first-detected microcracks are less than 1 μm in length. Specimens were cycled until failure. Fatigue life N_f was defined as the number of cycles at the point where a measurable drop (5%) in the ratio of maximum stress in tension to maximum stress in compression was detected. In order to study the effects of the oxide thickness and the strain amplitude, specimens with 0.6 μm thick oxide were cycled at $\Delta\varepsilon_p/2$ of 5×10^{-4} and 1×10^{-3} in air. After the cyclic plastic straining, a 30° taper section parallel to the gauge direction was prepared by polishing and etching for about 0.5 s with a 3% nital solution to visualize the crack propagation mode.

3. Results

As-polished HSLA steel specimens were cycled at $\Delta\varepsilon_p/2$ of 5×10^{-4} in air and in UHV. In the fatigue test in air, periodically spaced intrusions of ~0.2 μm length were observed after 8000 cycles (Fig. 1a). These intrusions lying on the slip band were later seen to grow to form a slip band crack as shown in Fig. 1b. Fatigue crack initiation along the prominent slip bands has also been reported for other HSLA steels [15, 16]. Slip bands and microcracks are not crystallographic due to the many slip systems available in this bcc material. Microcracks form only within a grain whose crystallographic orientation is favourable for slip. Surface deformation was very inhomogeneous from grain to grain and the integrity of the grain boundaries was maintained even at very late stages of fatigue life. Fatigue in UHV produces short and wavy slip-line microcracks inside a grain as in the case of the air test, but at a higher number of cycles in UHV (Fig. 2a). Little environment-induced differences were observed in the plastic surface deformation and the microcrack initiation features. Grain boundaries show a great resistance to the fatigue damage and act as effective barriers to the spreading of microcracks. The microcrack initiation life and the fatigue life in UHV are about five times and more than ten times longer than those in air, respectively. The environmental effect is greater in the microcrack growth stage than in the microcrack initiation stage. During the microcrack growth stage, the gaseous environment is responsible for most of the fatigue damage. The overall surface deformation at the late stage of fatigue life in UHV (Fig. 2b) is more severe and homogeneous than in air because of the higher accumulated plastic strain resulting from the longer fatigue life in UHV.

Specimens with a 0.2 μm thick wustite surface layer were cycled at $\Delta\varepsilon_p/2$ of 5×10^{-4} in air and in UHV. In contrast to the as-polished specimens, the intergranular initiation of fatigue cracks was the favoured mode. Fig. 3a shows an example of the intergranular cracking developed in the oxide layer after 10 000 strain cycles at 5×10^{-4} in air. The density of the intergranular cracks did not increase appreciably in number from this point to failure. Instead, microcracks already initiated were found to grow forming long intergranular cracks. Grain boundaries in the oxide layer could be identified without etching. It was also observed from SEM study that these grain boundaries coincide with those of the substrate. This is perhaps due to the varying oxidation rate of each grain according to the orientation of the substrate [17]. Transgranular cracks were hardly observed even after 20 000 cycles, the terminal stage of the cyclic lifetime (note that N_f is 22 500 cycles). Fig. 3b is a TEM micrograph of surface replica taken after 20 000 cycles, showing severe grain

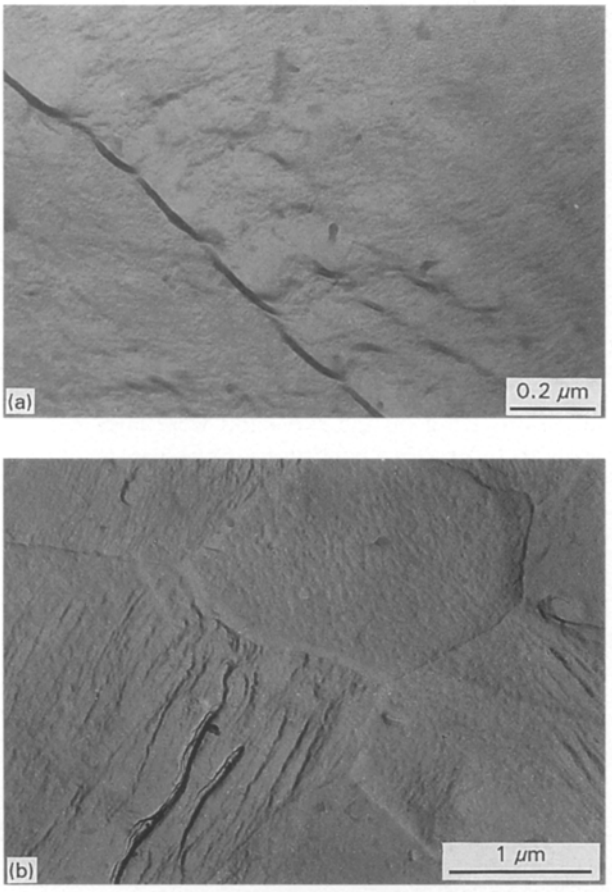

Figure 1 TEM micrographs of surface replica of as-polished HSLA steel cycled at $\Delta\varepsilon_p/2$ of 5×10^{-4} in air (a) after 8000 cycles, (b) after 15 000 cycles.

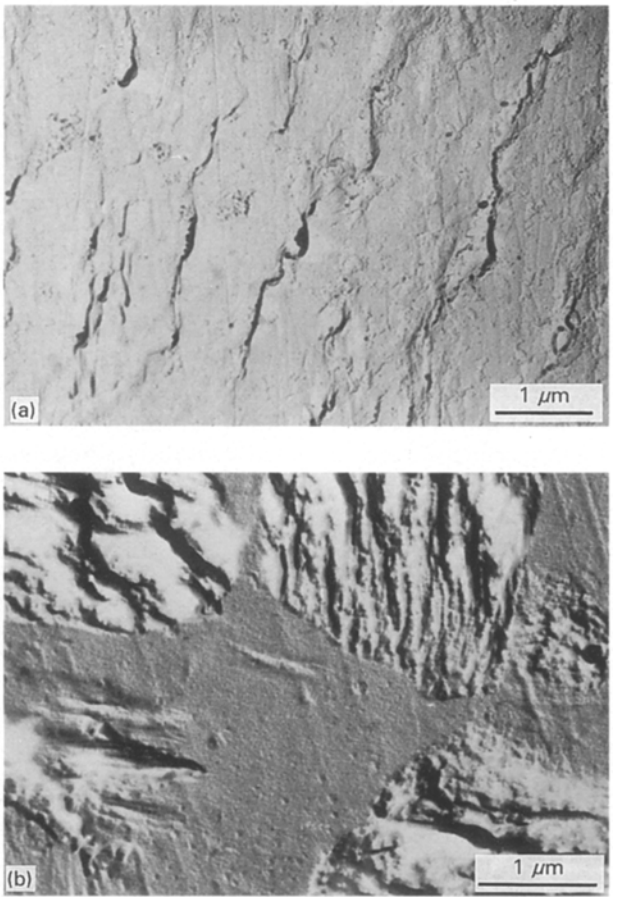

Figure 2 TEM micrographs of surface replica of as-polished HSLA steel cycled at $\Delta\varepsilon_p/2$ of 5×10^{-4} in UHV (a) after 65 000 cycles, (b) after 470 000 cycles.

boundary cracking. Fatigue in UHV also produces intergranular microcracks after 10 000 cycles, as shown in Fig. 4a. Microcrack initiation in the oxide layer was not affected by the environment. Once, however, cracking occurs in the surface oxide layer, active gases can attack the substrate through the crack path. Therefore, the fatigue life of an oxidized specimen in UHV is greatly extended due to the decrease of crack growth rate. Even after 500 000 cycles (which is already more than 20 times greater than the fatigue life in air), fatigue test in UHV showed no indication of fatigue failure. At this point, the number of cracks was greater compared to that in the terminal stage of the air test, but cracks extending more than two surface grains were hardly ever observed. Fig. 4b shows the surface of the oxidized specimen cycled 500 000 times in UHV. The observed intergranular cracks are oriented nearly normal to the strain axis. After reaching a triple point, the crack follows the second grain boundary segment lying closest to the normal to the strain axis.

As in the case of the 0.2 μm thick oxide layer specimen, the 0.6 μm thick oxide layer specimen fatigued at $\Delta\varepsilon_p/2$ of 5×10^{-4} favours grain boundary cracking. By increasing the oxide thickness from 0.2 to 0.6 μm, the number of cycles required for microcrack initiation N_i is greatly reduced. With the application of only 50 strain cycles, microcracks initiated along the valley between the facets of the thermally grown surface oxide (Fig. 5a). It presents a striking contrast to the crack initiation life for the as-polished specimen which is 8000–15 000 cycles under the same test condition. It is apparent that the 0.6 μm thick wustite layer is detrimental to fatigue microcracking in HSLA steel at this test condition. With continued cycling, more microcracks initiated and grew along the grain boundaries lying nearly normal to the strain axis. Fig. 5b is a scanning electron micrograph showing the post-fatigue surface after 19 000 cycles. It was found from SEM observation of the 30° taper section through the oxide layer that only grain boundary cracks penetrate into the substrate.

Significantly earlier formation of microcracks due to the presence of 0.6 μm thick oxide was observed at the higher plastic strain amplitude ($\Delta\varepsilon_p/2 = 1 \times 10^{-3}$). Fig. 6a shows microcracks initiated along the oxide grain boundaries, following the application of only 20 strain cycles. With continued cycling, transgranular cracks also developed after 1000 cycles. However, these transgranular cracks did not seem to grow appreciably. Fig. 6b shows the post-fatigue surface after 8000 cycles. Brittle fracture of the oxide is quite prevalent. Short and fine cracks are transgranular, while large and intensive cracks are intergranular. Transgranular cracks are also oriented nearly normal to the strain axis and independent of the crystallographic nature of the underlying metal, in agreement with those reported in earlier studies [18–20]. The density

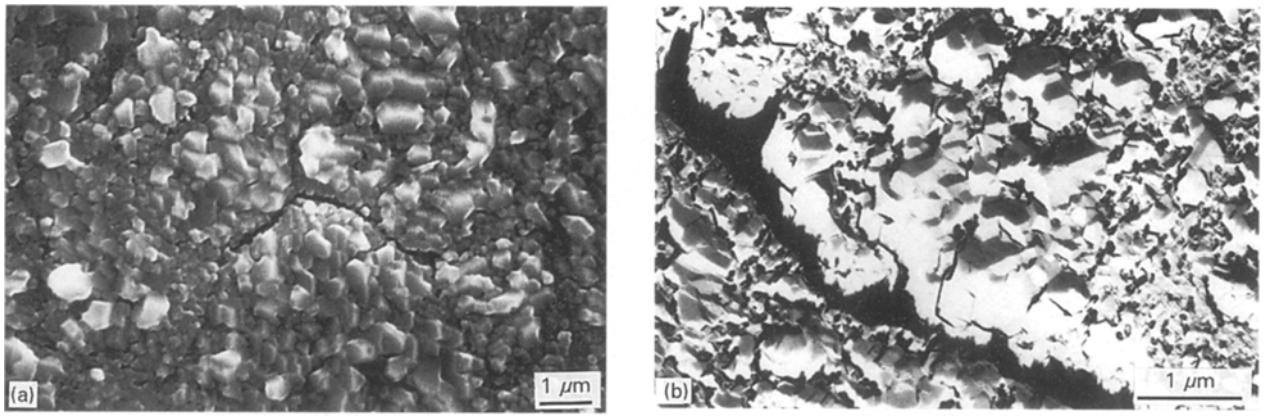

Figure 3 Surfaces of 0.2 μm thick wustite cycled at $\Delta\varepsilon_p/2$ of 5×10^{-4} in air (a) after 10 000 cycles, (b) after 20 000 cycles.

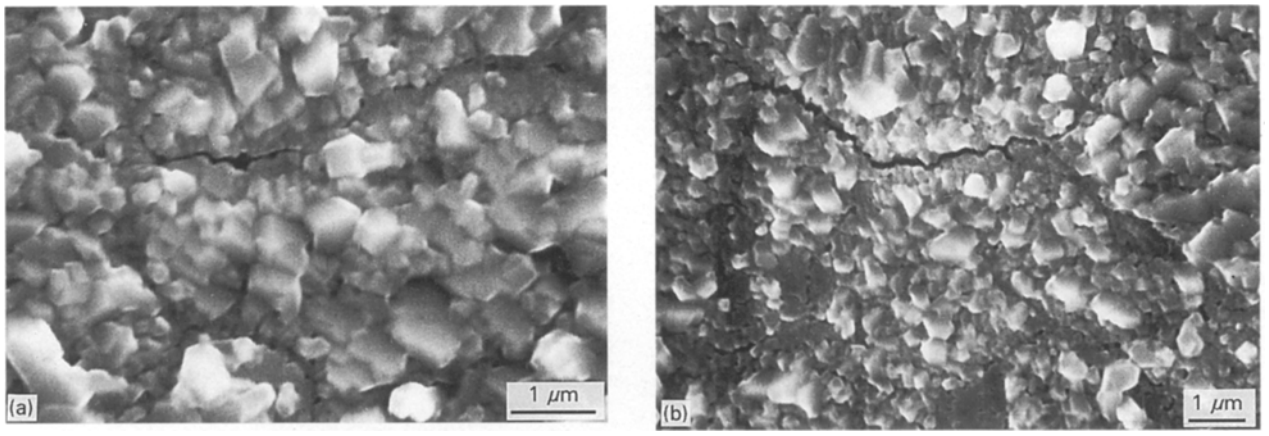

Figure 4 Surfaces of 0.2 μm thick wustite cycled at $\Delta\varepsilon_p/2$ of 5×10^{-4} in UHV (a) after 10 000 cycles, (b) after 500 000 cycles.

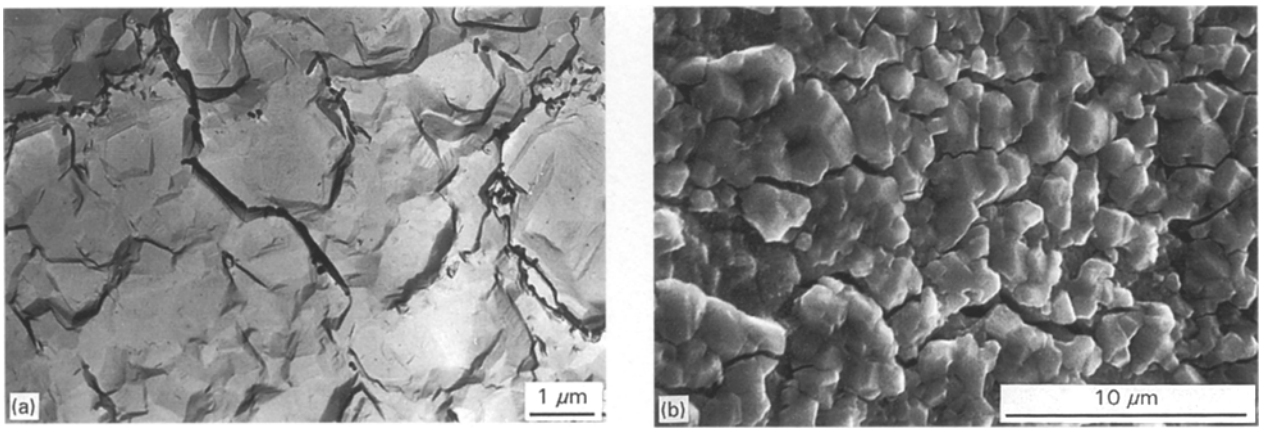

Figure 5 Surfaces of 0.6 μm thick wustite cycled at $\Delta\varepsilon_p/2$ of 5×10^{-4} in air (a) after 50 cycles, (b) after 19 000 cycles.

of cracks is higher in comparison to that at the lower plastic strain of 5×10^{-4}. In order to determine which cracking mode is responsible for final failure, a 30° taper section through the oxide layer after 8000 cycles was prepared and examined using an SEM. The scanning electron micrograph (Fig. 7) conclusively shows that only grain boundary cracks develop into the substrate while transgranular cracks fail to penetrate appreciably.

Microcracks in the oxide layer initiate earlier than those in the as-polished specimens. Intergranular microcracks initiate extremely early in the fatigue life with the thicker (0.6 μm) wustite surface layer at both strain amplitudes tested. Microcrack initiation life of the specimen with the thinner (0.2 μm) oxide layer is greater than that for the thicker oxide layer, but still smaller than that of the as-polished specimen. Microcrack initiation in the oxide layer is not affected by the gaseous environment. Once, however, the surface oxide fractures, further crack growth through the base metal is greatly suppressed in UHV. Graphical representation of N_i and N_f at $\Delta\varepsilon_p/2$ of 5×10^{-4} in air and in

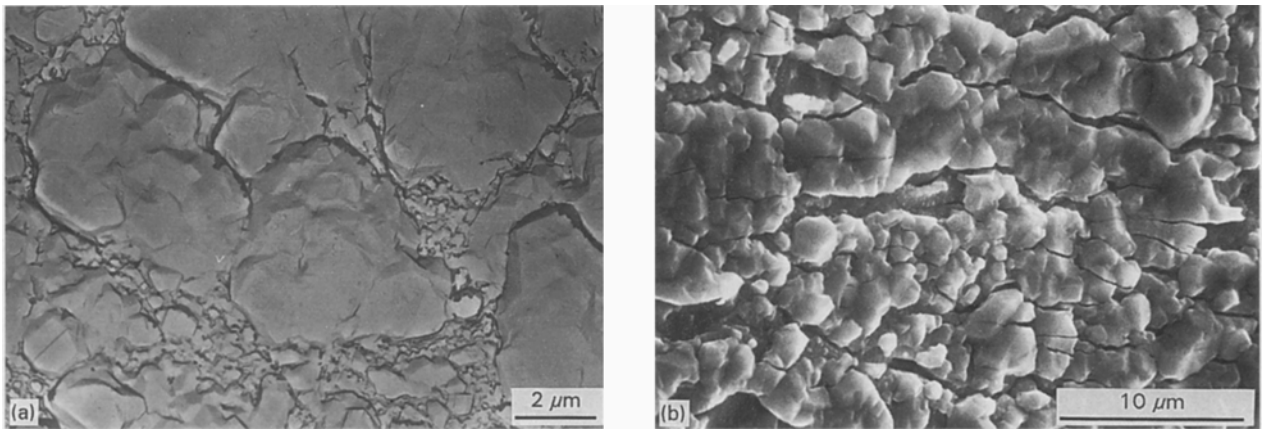

Figure 6 Surfaces of 0.6 μm thick wustite cycled at $\Delta\varepsilon_p/2$ of 1×10^{-3} in air (a) after 20 cycles, (b) after 8000 cycles.

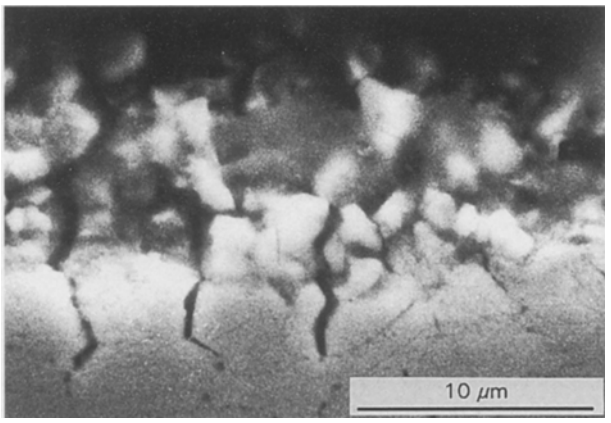

Figure 7 SEM micrograph of 30° taper section of the oxidized specimen cycled 8000 times at $\Delta\varepsilon_p/2$ of 1×10^{-3} in air. Wustite thickness is 0.6 μm.

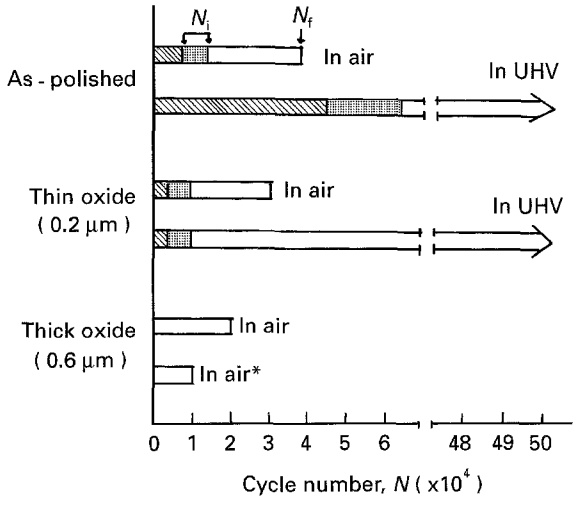

Figure 8 Graphical representation of fatigue crack initiation life (N_i) and fatigue life (N_f) at $\Delta\varepsilon_p/2$ of 5×10^{-4} in air and in UHV with as-polished and oxidized surfaces (*$\Delta\varepsilon_p/2 = 1 \times 10^{-3}$).

UHV with polished and oxidized surfaces is given in Fig. 8.

4. Discussion

Surface layers with physical properties different from those of the substrate affect the movement of the near-surface dislocations. The mechanism by which a surface layer affects the behaviour of the near-surface dislocations is related to the elastic interaction between dislocations and the surface layer, the different crystal structure or orientation of the surface layer with respect to the substrate, and the misfit strain accommodation at the interface. Considerable efforts have been made to find out the force that a surface covered with a film exerts on the near-surface dislocations [21–24]. A surface covered with a film whose shear modulus is greater than that of the substrate will exert a long range attractive force and a short range repulsive force. If the shear modulus of the film is smaller than that of the substrate, the force exerted on the dislocation by the surface is completely attractive. However, it should be noted that a surface film, regardless of its shear modulus, always suppresses the mobility of dislocations as compared with the case where a surface film does not exist. Hence, the film can act as a barrier to the dislocation emergence and suppress the surface plasticity. For the case of a wustite film on iron, the abrupt change in crystal structure from bcc (iron) to fcc (wustite) and the misorientation of slip planes across the interface serve as obstacles for dislocations to slip through the interface. Besides, the lattice misfit between wustite and iron (about 6% with respect to wustite) is expected to be accommodated by a two-dimensional grid of dislocations at the interface [25, 26]. This interfacial dislocation network may also serve as an effective barrier to glide. One may therefore suspect that the dislocations accumulate at the interface during strain cycling and that this dislocation pile-up causes the cracking of the oxide film [25].

In thermally oxidized specimens, intergranular cracking is always the favoured mode and leads to final failure regardless of the strain amplitude, the oxide thickness or the environment used in the present research. The intergranular failure is activated by the grain boundary microcracking in the surface oxide layer. With the application of less than 50 cycles in 5×10^{-4} and 20 cycles in 1×10^{-3} plastic strain cycling, grain boundary cracking was observed in the 0.6 μm thick oxide layer. It is unlikely that grain boundary sliding in the substrate occurs to a degree

significant enough to cause grain boundary cracking in the oxide overlayer with the application of less than 50 cycles at those strain amplitudes. (Remember that the grain boundaries of the oxide layer coincide with those of the substrate.) When the as-polished specimens were fatigued under the same test conditions, no significant grain boundary sliding was observed even at a much later stage of the cyclic lifetime. The growth rate of wustite varies appreciably from grain to grain according to the orientation of the iron substrate [17]. The thickness variation of the grown oxide of each grain could produce severe stress concentrations at grain boundaries, leading to a premature cracking. This occurs more severely as the oxide thickness increases, resulting in greater reduction in the crack initiation life of the thicker oxide specimen. Therefore, it is believed that the grain boundary cracking of the oxide layer is related not to the plastic deformation of the underlying substrate but to the total strain applied to the oxide layer itself.

It was observed that transgranular cracking becomes more prevalent for the wustite/HSLA steel specimen as the plastic strain amplitude increases. Working with wustite/polycrystalline iron specimens which have a similar wustite thickness and a greater grain size as compared to those of wustite/HSLA steel specimens used in the present research, a similar observation was reported by Cooper [27]. However, transgranular cracks were developed much earlier in the wustite/iron specimens than in the wustite/HSLA steel specimens at the same plastic strain amplitude. Considering that the total strain applied to the polycrystalline iron specimen is much smaller than that applied to HSLA steel at the same plastic strain amplitude, it is thought that transgranular cracking is related not to the total strain but to the plastic deformation of the underlying substrate. As discussed earlier, dislocations produced during the cyclic plastic straining are expected to accumulate just under the oxide/substrate interface. Grosskreutz and Bowles [28, 29] reported that edge dislocation dipoles were trapped just beneath the 5 ~ 10 nm thick aluminium oxide after cyclic straining of aluminium single crystals. As the plastic strain amplitude increases, a higher degree of dislocation multiplication and pile-up is expected. In comparison to the small grain size of HSLA steel, the larger grain size of iron leads to a greater dislocation pile-up at the interface. Therefore, the transgranular cracking in the brittle oxide surface layer is ascribed to an avalanching process of the dislocations piled up against the oxide interface. A transgranular microcrack initiates when the local stress due to the dislocation pile-up exceeds the fracture strength of the brittle oxide.

One of the important roles of a surface coating is to protect the base material against environmental attack. The effect of atmosphere can be effectively removed if the surface oxide layer is impervious or reduces the diffusion of gaseous elements. The role of the oxide layer as a protector is only effective as long as it remains intact. Fracture in the oxide film causes a preferential environmental attack to the exposed substrate. Moreover, it also creates stress concentration and provides preferential sites for the egress of dislocations [30]. For these reasons, when a surface film fractures, crack initiation in the substrate almost always occurs at the point of film fracture [18, 31]. As mentioned earlier, the intergranular fatigue cracking was predominant in the wustite/HSLA steel specimens. Major cracks leading to final failure were invariably found along the grain boundaries. While both transgranular and intergrannular cracks were developed at 1×10^{-3} plastic strain, intergranular cracks grew further into the substrate, while transgranular cracks failed to penetrate. There are factors that could help the preferential growth of the grain boundary cracking into the substrate. The impurities could be segregated at grain boundaries during the thermal oxidation, causing the embrittlement of grain boundaries. The penetration of the oxide into the grain boundaries during oxidation treatment may also be a contributing factor for the grain boundary cracking. Grain boundary cracks in the oxide layer allow a direct corrosive environmental attack on the grain boundary of the substrate, developing a fatal crack there.

Fig. 9 shows lifetimes at a plastic strain amplitude of 5×10^{-4} in air as a function of oxide thickness. Microcracks in the brittle oxide layer initiate very early in fatigue life compared to the as-polished condition. The thicker oxide, in particular, caused a considerable reduction in the microcrack initiation life. However, microcrack growth life (N_f–N_i) is affected less. Working with iron coated with wustite, Cooper [27] also found that microcracks initiate earlier in the thicker oxide than in the thinner oxide in the low cycle fatigue test at $\Delta\varepsilon_p/2$ of 5×10^{-4}. Stickley and Lyst [32] also observed detrimental effects of thick anodic coatings on the fatigue strength in aluminium alloys at a relatively high stress, presumably due to the premature microcracking of the brittle coating. On the other hand, a beneficial effect of an oxide film was reported in the high-cycle test by Grosskreutz [30] who found that crack initiation life of the aluminium specimen

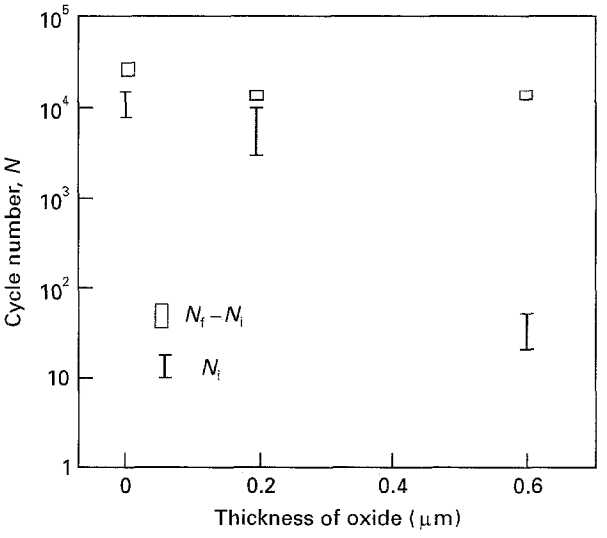

Figure 9 Fatigue crack initiation life (N_i) and crack growth life (N_f–N_i) at $\Delta\varepsilon_p/2$ of 5×10^{-4} in air as a function of oxide thickness.

coated with a 0.15 μm thick aluminium oxide is more than three times greater in comparison to the as-polished condition. According to the calculation of the elastic interaction force on near-surface dislocations, a thicker surface film makes dislocations less active near the interface than a thinner film. Since a thicker oxide exerts a smaller attractive force (or larger repulsive force) on the near-surface dislocations than a thinner oxide, the number of dislocations reaching the interface is correspondingly reduced and the surface deformation is also suppressed. Furthermore, the thicker oxide may be more effective in protecting the substrate from the corrosive environment. Therefore, one may expect that the fatigue crack initiation and growth are delayed more effectively by the presence of the thicker oxide film. However, the beneficial effect of an oxide layer to suppress fatigue crack initiation is true only as long as it remains intact. Under the condition where the brittle oxide easily fractures, such as in high-strain-amplitude low-cycle tests, the presence of the oxide layer can even be harmful, as observed in the present research. In conclusion, it should be emphasized that the effects of an oxide layer on the fatigue strength depends critically on the test condition and on the ability of the oxide layer to maintain its integrity.

5. Conclusions

The effects of a well-characterized wustite ($Fe_{0.94}O$) surface layer thermally grown to 0.2 and 0.6 μm thicknesses on fatigue crack initiation and growth in HSLA steel was studied at $\Delta\varepsilon_p/2$ of 5×10^{-4} and 1×10^{-3} in air and in UHV. In the as-polished condition, slip-band cracking is the favoured mode at $\Delta\varepsilon_p/2$ of 5×10^{-4} both in air and in UHV. The number of cycles to initiate a fatigue microcrack as well as the number of cycles to the failure are larger in UHV than those in air. The increase in fatigue resistance in UHV is attributed mainly to the decrease in the microcrack growth rate. Specimens with a wustite surface layer show predominantly intergranular cracking both in air and in UHV. Transgranular cracks appear in the oxide layer at a high plastic strain amplitude of 1×10^{-3}, but they fail to propagate appreciably into the base metal. Intergranular microcracking is related to the total strain applied to the oxide layer. Transgranular cracking in the brittle oxide layer is related to the plastic deformation of the underlying substrate, and it is ascribed to the avalanching process of dislocations piled up against the oxide interface. Microcrack initiation in the oxide layer is not affected by the environment. Once, however, the surface oxide fractures, the crack growth rate through the base metal is greatly reduced in UHV.

Acknowledgements

The authors would like to thank Dr M. E. Fine for many helpful discussions and Dr S. P. Bhat and R. Cline of Inland Steel Research Laboratory for providing oxidized samples.

References

1. R. ROSCOE, *Phil. Mag.* **21** (1936) 399.
2. V. K. SETHI and R. GIBALA, in "Surface Effects in Crystal Plasticity", edited by R. M. Latanision and J. T. Fourie, NATO Advanced Study Institute Series, Series E, (Noordhoff, Leyden, 1977) p. 599.
3. H. J. GOUGH and D. G. SOPWITH, *J. Inst. Metals* **49** (1932) 93.
4. *Idem, ibid.* **52** (1935) 55.
5. C. M. HUDSON and S. K. SEWARD, *Eng. Frac. Mech.* **8** (1976) 315.
6. B. I. VERKIN and N. M. GRINBERG, *Mater. Sci. Eng.* **41** (1979) 149.
7. R. WANG, H. MUGHRABI, S. McGOVERN and M. RAPP, *ibid.* **65** (1984) 219.
8. D. MAJUMDAR and Y. W. CHUNG, *Scripta Metall.* **16** (1982) 791.
9. C. LAIRD and G. C. SMITH, *Phil. Mag.* **8** (1963) 1945.
10. P. S. MAIYA, *Scripta Metall.* **9** (1975) 1141.
11. *Idem, ibid.* **11** (1977) 331.
12. W. J. LEE, S. P. BHAT, Y. W. CHUNG and M. E. FINE, in Proceedings of the 3rd International Conference on Fatigue and Fatigue Thresholds: Fatigue '87, Vol. III, Charlottesville, June 1987, edited by R. O. Ritchie and E. A. Starke, Jr (EMAS, UK, 1987) p. 1211.
13. D. MAJUMDAR, Ph. D. Diss., Dept. of Materials Sci. and Eng., Northwestern University, 1983.
14. W. J. LEE, J. P. BAKER, Y. W. CHUNG and M. E. FINE, *Rev. Sci. Instrum.* **57** (1986) 2854.
15. Y. H. KIM and M. E. FINE, *Met. Trans.* **13A** (1982) 59.
16. G. GONZALEZ and C. LAIRD, *ibid.* **14A** (1983) 2507.
17. R. F. MEHL and E. F. McCANDLESS, *Trans. AIME* **125** (1937) 531.
18. G. A. BEITEL and E. Q. BOWLES, *J. Metal Sci.* **5** (1971) 85.
19. W. J. BAXTER and S. R. ROUZE, *J. Appl. Phys.* **49** (1978) 4233.
20. T. K. G. SWAMI, Ph.D. Diss., Dept. of Materials Sci. and Eng., Northwestern University, 1981.
21. A. K. HEAD, *Phil. Mag.* **44** (1953) 92.
22. *Idem, Australian J. Phys.* **13** (1960) 278.
23. G. H. CONNERS, *Int. J. Eng. Sci.* **5** (1967) 25.
24. R. WEEKS, J. DUNDURS and M. STIPPES, *Inst. J. Eng. Sci.* **6** (1968) 365.
25. C. V. COOPER and M. E. FINE, *Met. Trans.* **16A** (1985) 641.
26. J. S. VERMAAK and J. H. van der MERWE, *Phil. Mag.* **10** (1964) 785.
27. C. V. COOPER, Ph.D. Diss. Dept. of Materials Sci. and Eng., Northwestern University, 1983.
28. J. C. GROSSKREUTZ, *Surf. Sci.* **8** (1967) 173.
29. J. C. GROSSKREUTZ and C. Q. BOWLES, in "Environment-Sensitive Mechanical Behavior", edited by A. R. C. Westwood and N. S. Stoloff (Gordon and Breach, New York/London, 1966) p. 67.
30. J. C. GROSSKREUTZ, in "Corrosion Fatigue", NACE-2 (1972) p. 201.
31. R. G. GATES and W. A. WOOD, *J. Inst. Metals* **96** (1968) 242.
32. G. W. STICKLEY and J. O. LYST, *J. Mater.* **1** (1966) 19.

Received 8 September 1993
and accepted 24 August 1994